Forced Rossby Waves in Observed Background Flows

J. EGGER

Meteorologisches Institut, Universität München, Federal Republic of Germany

(Manuscript received 22 April 1987, in final form 14 January 1988)

ABSTRACT

We consider forced quasi-stationary Rossby waves in background flows with realistic variability in time and space. Long-term integrations of the nonlinear barotropic vorticity equation for deviations from background flow are carried out where a forcing term provides sources and sinks of vorticity for the deviations. The background flow is specified according to daily flow observations at 300 hPa. Mean deviation patterns for individual months and for the total period on record (18 months) are computed and compared to the results of more conventional linear and nonlinear computations where a zonal background flow is essentially fixed in time. It is the purpose of this paper to estimate the impact of the variability of the background flow in computations of quasi-stationary Rossby waves. For how long must a forcing act to make the application of linear theories to the response promising? Results are sensitive to the choice of the surface friction parameter C and eddy diffusivity D. For $C = 1/(10 \text{ days})$, $D = 1 \times 10^5 \text{ m}^2 \text{ s}^{-1}$ there are considerable discrepancies of computed monthly means and the corresponding solutions for fixed background flow. There is good agreement, however, if averages over the complete period of integration are compared. This suggests that conventional linear theories can be applied to climatological stationary waves. The variability of the background flow cannot be neglected, however, if events of only a few months duration are considered.

1. Introduction

Theoretical work on quasi-stationary Rossby waves is mainly motivated by the desire to explain the observed monthly or seasonal mean planetary wave patterns as a response to various forcing mechanisms. For example, it has been proposed that the observed quasi-stationary waves in the troposphere and stratosphere are induced by orographic forcing and by heat sources (e.g., Charney and Eliassen 1949; Smagorinsky 1953; Jacqmin and Lindzen 1985). It has also been suggested that anomalous forcing like that due to anomalies of the sea surface temperature distribution may cause anomalous wave responses (e.g., Egger 1977; Gill 1980). In linear theories, in particular, one looks at these waves as perturbations of a basic state which represents the atmospheric long-term mean state which may depend on height and latitude (see Held 1983 for a review of relevant work). Even longitude-dependent background flows have been considered (e.g., Simmons et al. 1983).

It is, however, a generally accepted simplification to choose basic flows that do not depend on time. This choice is partly motivated by mathematical convenience. It is easier to study wave propagation in a constant mean flow than in a time-dependent environment. In addition it is hoped that the perturbations caused by the variability of the background flow will be small when long-term averages are considered.

The equations of atmospheric motions state, however, that motions of all frequencies ω influence the slow part of the spectrum ($|\omega| < \omega_s$, for example, with $\omega_s = 2\pi/\text{month}$) where the quasi-stationary waves reside. It is at least not obvious that this interaction can be neglected. Quite to the contrary one can argue that part of the observed variability of the quasi-stationary waves is due to this interaction (Egger and Schilling 1983; see also Simmons et al. 1983, who list the influence of shorter-term transients on the forced slow response as a remaining problem). This problem becomes even more serious when we consider the response to anomalous forcing where the phenomena to be studied hardly persist for longer than a month or a season. Are we justified in neglecting the changes of the atmospheric circulation during an anomalous forcing episode when computing the quasi-stationary response to this anomalous source? Of course, there is no generally valid answer to such questions.

In this paper we want to consider barotropic flows on the sphere. We conduct experiments where a localized source of vorticity is prescribed. Orographic forcing is considered as well. It is mainly for the sake of simplicity that we have chosen just this problem. Although baroclinic problems may be even more interesting and rewarding it appears reasonable to tackle the simpler situation first. Long-term integrations of the nonlinear-vorticity equation for deviations ψ_d from a background flow ψ_b are carried out. The background

Corresponding author address: Dr. J. Egger, Meteorologisches Institut der Universität München, Theresienstraße 37, 8000 München 2, Federal Republic of Germany.

flow is specified according to daily flow observations at 300 hPa. Time averages $\bar{\psi}_d^T$ over an interval T are computed and compared to corresponding solutions where the time-dependence of the background flow is neglected. This procedure will provide some information on the relative importance of the variability of the background flow to time averages of the response.

2. The model

The barotropic vorticity equation on the sphere reads

$$\frac{\partial}{\partial t}(\nabla^2 - \delta^{-2})\psi + J(\psi, \nabla^2\psi + 2\Omega \sin\varphi) = -C\nabla^2\psi + D\nabla^4\psi + F \quad (2.1)$$

where ψ is the streamfunction of barotropic planetary flow, δ a radius of deformation, Ω the earth's rotation rate, and φ latitude. Following Egger and Schilling (1983) we choose $\delta = 10^6$ m. The first term on the right-hand side of (2.1) represents surface friction with a damping constant C. The second term describes horizontal diffusion of vorticity by subgrid motions with an eddy diffusivity D. The forcing is denoted by F.

We split the streamfunction

$$\psi = \psi_b + \psi_d \quad (2.2)$$

into a background part ψ_b and a deviation ψ_d therefrom. Since we are concerned with Rossby waves we assume that ψ_d consists of waves only: $\bar{\psi}_d^\lambda = 0$; $\psi_d = \psi_d(\lambda, \varphi, t)$, where λ is longitude and the symbol $(\bar{}^\lambda)$ stands for an average over longitude. The background flow contains a zonal part as well as a wave component

$$\psi_b = \psi_{bz}(\varphi, t) + \psi_{bw}(\lambda, \varphi, t) \quad (2.3)$$

with $\bar{\psi}_{bw}^\lambda = 0$. We have to choose ψ_b such that the background flow has a realistic variability in time (and space). One may be able to satisfy this requirement by developing a stochastic model for the background flow. This is a difficult problem which has not been solved yet. However, it is much easier to use observations to specify ψ_b. In that case we are certain that the background flow is "realistic."

We split the forcing

$$F = F_b + F_d \quad (2.4)$$

where F_b is defined such that ψ_b satisfies (2.1) with $F = F_b$. Thus

$$F_b = \frac{\partial}{\partial t}(\nabla^2 - \delta^{-2})\psi_b + J(\psi_b, \nabla^2\psi_b + 2\Omega \sin\varphi) + C\nabla^2\psi_b - D\nabla^4\psi_b. \quad (2.5)$$

The equation for ψ_d is derived by inserting (2.2), (2.4), and (2.5) in (2.1):

$$\frac{\partial}{\partial t}(\nabla^2 - \delta^{-2})\psi_d + J(\psi_d, \nabla^2\psi_b + 2\Omega \sin\varphi) + J(\psi_b, \nabla^2\psi_d) + (1-\gamma)J(\psi_d, \nabla^2\psi_d) = -C\nabla^2\psi_d + D\nabla^4\psi_d + F_d. \quad (2.6)$$

Equation (2.6) is linear in ψ_d for $\gamma = 1$ (provided F_d is linear) and becomes a nonlinear equation for $\gamma = 0$. We wish to emphasize that we do not consider deviations ψ_{dz} of the zonal flow. On principle, all Jacobians in (2.6) could create such deviations. However, we restrict our attention to the wavy part of the deviation field.

Given a forcing F_d we want to compute the quasi-stationary response $\bar{\psi}_d^T$ to this forcing where the symbol $(\bar{}^T)$ stands for a time average over a period of length T. The mean deviation $\bar{\psi}_d^T$ is governed by the time average of (2.6):

$$(\nabla^2 - \delta^{-2})[\psi_d(t+T) - \psi_d(t)]/T + J(\bar{\psi}_d^T, \nabla_b^2\bar{\psi}^T + 2\Omega \sin\varphi) + J(\bar{\psi}_b^T, \nabla^2\bar{\psi}_b^T) + (1-\gamma)J(\bar{\psi}_d^T, \nabla^2\bar{\psi}_d^T) = -C\nabla^2\bar{\psi}_d^T + D\nabla^4\bar{\psi}_d^T + F_t + \bar{F}_d^T \quad (2.7)$$

where

$$F_t = -\overline{J(\psi'_d, \nabla^2\psi'_b)}^T - \overline{J(\psi'_b, \nabla^2\psi'_d)}^T - (1-\gamma)\overline{J(\psi'_d, \nabla^2\psi'_d)}^T \quad (2.8)$$

and $\psi' = \psi - \bar{\psi}^T$. The term F_t represents the so-called transient eddy forcing. Given a forcing F_d which varies little with time we anticipate that pronounced differences of $\bar{\psi}_d^T$ from month to month, say, are mainly due to the variability of F_t with time. Note, however, that F_t is determined through the integration of (2.6) in time. Unlike F_d it is not prescribed.

It remains to specify the forcing F_d of the deviation flow. Obviously we can only prescribe an idealized forcing for the deviation flow since the total influence of the real sources like the earth's topography is embodied in the background flow ψ_b. In this paper we consider two types of forcing. First we prescribe a localized forcing which depends neither on time nor on ψ_b. One may identify this forcing with an anomaly of the divergent wind assumed to be constant: $F_d = -f\nabla \cdot \mathbf{v}_2$. Second we examine orographic forcing:

$$F_d = -J(\psi_b + \psi_d, 2\Omega \sin\varphi_0 h/H). \quad (2.9)$$

In (2.9), h is the height of an idealized mountain localized at latitude $\varphi_0 = 33°$N and $H = 8000$ m is a scale height. The term $J(\psi_d, 2\Omega \sin\varphi_0 h/H)$ in (2.9) describes the interaction of the deviation flow with the mountain. Strictly speaking this is not a forcing term. However, we wish to include this interaction just as we include the term $J(\psi_d, \nabla^2\psi_d)$ in (2.6).

The numerical structure of the model is as follows. We use a spectral representation,

$$\psi_d = \sum_{m=1}^{M}\sum_{r=1}^{R} \psi_{m+r}^m P_{m+r}^m(\sin\varphi)\exp(im\lambda), \quad (2.10)$$

of the streamfunction, where $P^m_{m+r}(\sin\varphi)$ are associated Legendre polynomials. The pseudospectral method is used where multiplications are carried out in a grid with 24 Gaussian grid points between the poles. The truncation in (2.10) is rectangular with ten wavenumbers in longitude ($M = 10$) and ten wavenumbers $R = M$ in lateral direction. The daily data for this work were provided by the European Centre for Medium Range Weather Forecasts in a 17 by 17 triangular truncation. The streamfunction at 300 hPa was derived from the original set of wind data by computing the vorticity and inverting the Laplacian. We discard all those expansion coefficients $\psi^m_{b,m+r}$ of the observed background flow which are outside the resolution of the model. Data for the seven winters 1979/80 through 1985/86 form the basis for the experiments. The dataset for each winter begins on 20 November and ends on 8 March. A typical experiment is carried out as follows: We start the integration of (2.6) for each winter on 20 November. We choose $\psi_d = 0$ initially and the forcing induces deviations. We begin to evaluate the runs on 1 December. The model is run throughout the winter and we count the days in March as belonging to February. This procedure is carried out for all six winters on record. Next we compute long-term mean fields $\bar{\psi}^T_d$. Then we can specify our problem in more precise terms. Do these means change if we replace $\psi_b(\lambda, \varphi, t)$ in (2.6) by the time-independent mean $\bar{\psi}^T_b(\lambda, \varphi)$ or even by the zonally averaged basic state $\bar{\psi}^T_{bz}(\varphi)$? How does $\bar{\psi}^T_d$ compare to the linear solution? To answer these questions we simply have to compare pairs of long-term integrations of (2.6).

We use the following options for intercomparisons. First we prescribe the monthly mean $\psi_b = \bar{\psi}^1_{bz}$ ($T = 1$ month) in a long-term integration of the linear version ($\gamma = 1$) of (2.6). We update $\bar{\psi}^1_{bz}$ at the beginning of the corresponding month. This change of the zonal mean wind during the integration induces a weak transience. We assign the index $i = 1$ to this experiment. We repeat this experiment ($i = 2$) with the nonlinear vorticity equation ($\gamma = 0$). In a third experiment ($i = 3$) we prescribe $\psi_b = \psi_{bz}(\varphi, t)$. We update ψ_{bz} every day according to the observations. An intercomparison of experiments 2 and 3 will help to decide if time variations of the zonally averaged flow are of importance to the generation of quasi-stationary waves. Next ($i = 4$) we prescribe $\psi_b = \bar{\psi}^1_b(\lambda, \varphi)$ and finally we look at the general case $\psi_b = \psi_b(\lambda, \varphi, t)$ ($i = 5$). The updating of the observed fields is done at the first day of a month in experiment 4 and every day in experiment 5. Occasionally a parallel experiment to experiment 5 ($i = 6$) will be carried out where we simply change the sign of the forcing. It appears that the experiments $i = 3$ and $i = 5$ are novel and, therefore, of main interest. On the other hand work by Simmons et al. (1983), Branstator (1983) and others on wave propagation in mean flows which vary with longitude is closely related to experiment 4.

The intercomparison of the experiments is not a trivial matter since each experiment yields 18 monthly mean fields. In addition we obtain the sample mean $\bar{\psi}^{18}_d$ of the total period of integration. Of course, visual inspection of the fields provides the most helpful method for evaluation. The pattern correlation coefficient $p_L(p)$ relates a monthly mean field to the sample mean of the linear experiment (sample mean of the same experiment). More detailed statistical intercomparisons of the various experiments are based on the test proposed by Preisendorfer and Barnett (1983, to be referred as PB-test). This test is designed for problems like ours where the sample size is fairly small. Typical test variables are evaluated as follows. For every month with index j in an experiment with index q we represent the monthly mean deviations on a global grid with 24 points in latitude and 30 points in longitude. Then we read off monthly mean values $\bar{\psi}^1_{dq}(j, k)$ from squares containing nine grid points (see Fig. 4). We assign an index k ($1 \leq k \leq K = 9$) to these points and define a data cloud $D_q = [\bar{\psi}^1_{dq}(j, k); j = 1, 18; k = 1, K]$. This data cloud must be compared to the cloud D_c obtained in a second experiment with index c for the same grid points. Following PB we define a normalized mean distance

$$d(q, c) = 18 \sum_{j=1}^{18} \sum_{k=1}^{9} [\bar{\psi}^1_{dq}(j, k) - \bar{\psi}^1_{dc}(j, k)]^2 / \sigma_q \sigma_c \tag{2.11}$$

of the clouds where σ_q, σ_c are the scatters

$$\sigma^2 = \sum_{j=1}^{18} \sum_{k=1}^{9} [\bar{\psi}^1_d(j, k) - \bar{\psi}^{18}_d(k)]^2. \tag{2.12}$$

In the PB-test $d(q, c)$ is compared to a distribution of distances obtained by mixing the two data clouds and forming new pairs of clouds at random. If $d(a, b)$ is larger than a certain threshold obtained from this distribution we can state that the experiments q and c are different at the 95% level with respect to distance evaluation. The reader is referred to Preisendorfer and Barnett (1983) for further details. Another test variable is the spread

$$s(q, c) = (\sigma_q - \sigma_c)^2 / (\sigma_q \sigma_c). \tag{2.13}$$

In addition we evaluate the "deviation energy"

$$E = \frac{1}{2} \sum_{m=1}^{M} \sum_{r=1}^{M} (m + r)(m + r + 1) |\psi^m_{d,m+r}|^2 / a^2 \tag{2.14}$$

where a is the radius of the earth. We denote the energy of monthly mean fields by $E(\bar{\psi}^1_d)$, that of daily fields by $E(\psi_d)$ and the energy of the sample mean field by $E(\bar{\psi}^{18}_d)$.

It remains to specify the frictional parameters C and D. For the former we choose $C = 1/(10 \text{ days})$. If we choose large values of D we can suppress almost any

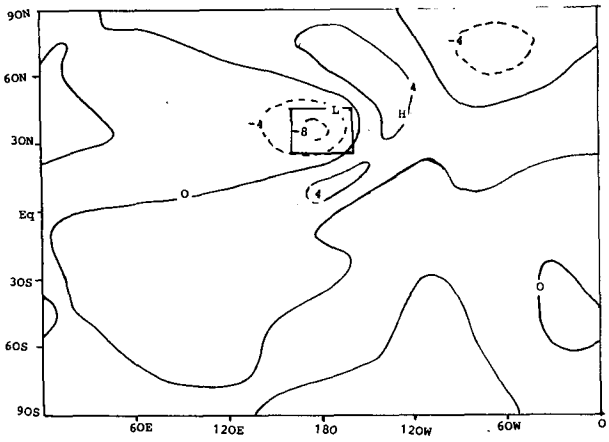

FIG. 1. Sample mean streamfunction $\bar{\psi}_d^{18}$ (10^6 m^2 s^{-1}) as obtained by averaging over all 18 monthly means of the linear experiment 1 ($\psi_b = \bar{\psi}_{bz}^1(\varphi)$; $\gamma = 1$; $D = 1 \times 10^5$ m^2 s^{-1}) for a localized vorticity source in the central Pacific (rectangle). Isoline distance is 4×10^6 m^2 s^{-1}; negative values dashed.

kind of development in the numerical experiments. On the other hand, if we prescribe $D \sim 0$ $E(\psi_d)$ may become unrealistically large (see also Fig. 15). In most experiments we choose $D = 1 \times 10^{-5}$ m^2 s^{-1}. Experiments with stronger damping $D = 5 \times 10^5$ m^2 s^{-1} have been performed as well.

3. Localized source of vorticity

We prescribe a source of vorticity situated in the central Pacific with a maximum strength of 1, 2 ($\times 10^{-10}$ s^{-2}) at its center (Fig. 1). The source's length is 3000 km, its width is 2000 km. We perform the experiments 1, 4, 5, 6, for this case.

a. *Experiment 1:* $\bar{\psi}_{bz}^1$; $\gamma = 1$; $D = 1 \times 10^5$ m^2 s^{-1}

In Fig. 1 we show the linear sample mean response to the forcing. Near the source we have the familiar picture of an upstream trough and an arc-shaped ridge in the lee. Wave amplitudes are 4–8 ($\times 10^6$ m^2 s^{-1}) near the source. Thus the amplitude of the response is weaker than that of the observed quasi-stationary waves. A visual inspection of individual monthly means reveals a strong similarity to Fig. 1 which is reflected in large values of the pattern correlation coefficient p (Table 1). Note that $E(\psi_d) > E(\bar{\psi}_d^{18})$ so that there is at least some transience.

b. *Experiment 4:* $\bar{\psi}_b^1(\lambda, \varphi)$; $\gamma = 0$; $D = 1 \times 10^5$ m^2 s^{-1}

The sample mean is less energetic than in experiment 1 (see Table 1) when we prescribe a zonally varying background flow. The upstream trough has just one closed isoline and the downstream ridge is less pronounced than in Fig. 1. The pattern correlation of this sample mean with Fig. 1 is as high as 0.87. However, individual monthly means may differ considerably from the corresponding linear fields (Table 1) so that the transient eddy forcing is not negligible in this experiment. As an example we show in Fig. 2a the mean for January 1983 where the response to the source is quite weak. With p_L eventually as low as 0.52 (Table 1) the linear theory as represented by experiment 1 would be of only moderate help in explaining the monthly means obtained in experiment 4. This statement is corroborated by the PB-test which indicates that experiments 1 and 5 differ almost everywhere.

c. *Experiment 5:* $\psi_b(\lambda, \varphi, t)$; $\gamma = 0$; $D = 1 \times 10^5$ m^2 s^{-1}

The energy level of the daily deviation fields is increased considerably when the most general background flow is prescribed (Table 1). With $E(\psi_d) = 58$ m^2 s^{-2} we obtain a perturbation field which has about one-fourth of the energy of the observed flow. The perturbations induced by the forcing are able to draw considerable amounts of energy from the time-varying background flow. The monthly mean fields are more energetic than in experiments 1, 4 and show a much larger variability. Thus we have now a pronounced transient eddy forcing. The correlation with the linear theory is poor for monthly means. For example, the monthly mean for January 1983 (Fig. 2b) shows virtually no resemblance to Fig. 1. The sample mean (Fig. 3), however, contains little energy and is reasonably well correlated with Fig. 1 ($p_L = 0.77$). Thus the linear theory yields useful results if the averaging period T is long enough. On the other hand, the linear theory is incapable of capturing details like the strong ridge to the east of the source in Fig. 3.

d. *Experiment 6:* $\psi_b(\lambda, \varphi, t)$; $\gamma = 0$; $D = 1 \times 10^5$ m^2 s^{-1}; sign of source changed

We repeat experiment 5 but change the sign of the source. Through this test we assess the impact of non-

TABLE 1. Average energies in (m^2 s^{-2}) of the daily fields $E(\psi_d)$, of the monthly means $E(\bar{\psi}_d^1)$ and the energy of the sample mean $E(\bar{\psi}_d^{18})$ and the range of the pattern correlation coefficients p and p_L in the experiments with a localized vorticity source.

Experiment	$E(\psi_d)$	$E(\bar{\psi}_d^1)$	$E(\bar{\psi}_d^{18})$	p	p_L
1	7	7	6	$0.88 \leq p \leq 0.97$	—
4	7	7	4	$0.61 \leq p \leq 0.88$	$0.52 \leq p_L \leq 0.94$
5	58	12	4	$0.37 \leq p \leq 0.84$	$0.13 \leq p_L \leq 0.80$
6	51	10	4	$0.46 \leq p \leq 0.87$	$0.15 \leq p_L \leq 0.71$

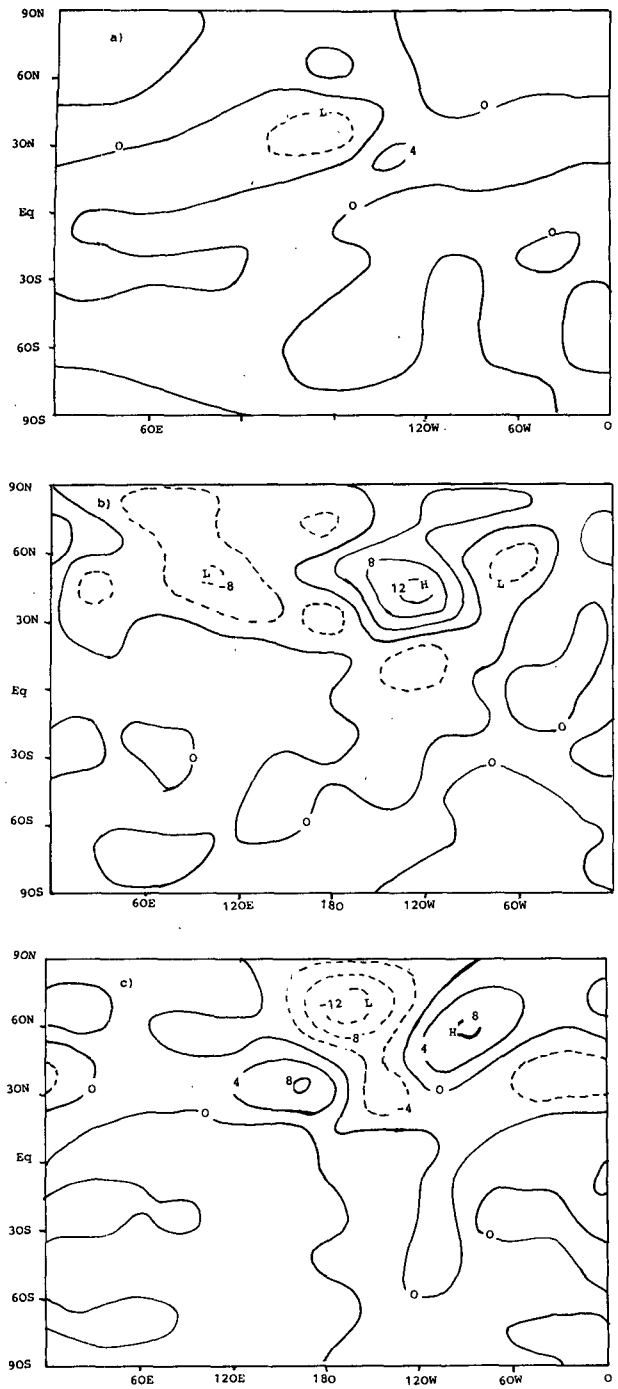

FIG. 2. Monthly mean streamfunction $\bar{\psi}_d^1$ (10^6 m^2 s^{-1}) for January 1983 in experiments with a localized vorticity source. (a) Experiment 4, (b) experiment 5, (c) experiment 6.

linearity in the presence of time-dependent background flows. The energy levels in this experiment are somewhat lower than in experiment 5 (Table 1). The sample mean field (not shown) correlates well with Fig. 1 ($p = -0.79$); however, individual monthly means cannot at all be obtained from those of experiment 5 by a change of sign. For example, the monthly mean for January 1982 (Fig. 2c) is by no means the reverse of Fig. 2b. A detailed intercomparison of experiments 5 and 6 is provided by the PB-test (Fig. 4). It is seen that there is little difference in the eastern hemisphere but the experiments tend to differ near the source and near the poles. Note that some of the dots and crosses in Fig. 4 come out by chance. The PB-test is repeated 80 times in Fig. 4. Since a 95% probability is assigned to each result we have the uncertainty that some of the symbols may disappear and a few new ones may appear if we repeat the procedure. Figure 4 suggests that differences like those between Fig. 2b and Fig. 2c are essentially due to the random development of ψ_d in variable background flow and not to nonlinearity alone.

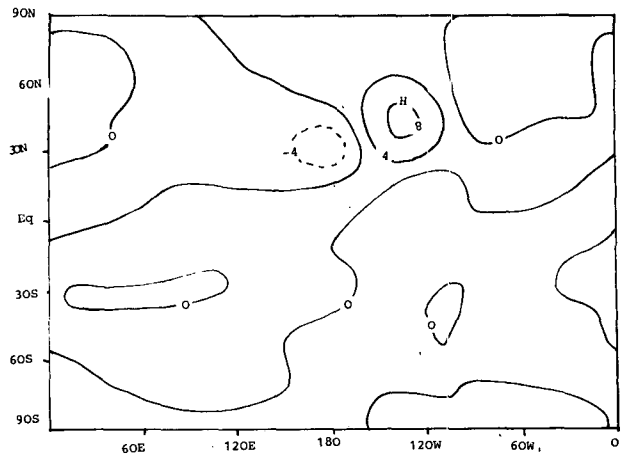

FIG. 3. Sample mean streamfunction $\bar{\psi}_d^{18}$ (10^6 m^2 s^{-1}) in experiment 5 [$\psi_b = \psi_b(\lambda, \varphi, t)$; $\gamma = 0$; $D = 1 \times 10^5$ m^2 s^{-1}] with a localized vorticity source.

4. Orographic forcing

We insert a sinusoidally shaped mountain massif of Himalayan scale in the flow (Fig. 5). The obstacle's length is 3000 km, the width is 2000 km and the max-

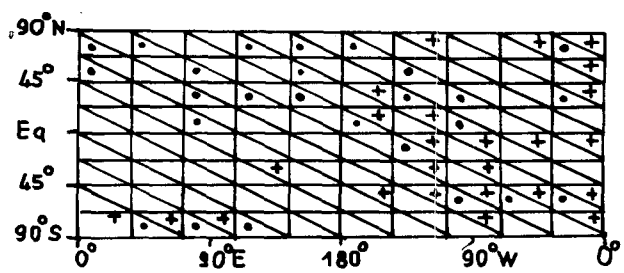

FIG. 4. Intercomparison of the 18 monthly means of experiments 5 and 6 (localized vorticity source) on the basis of the PB-test. To perform the test, the sign of ψ_b in experiment 6 has been reversed. If the experiments differ at the 95% level in a subsection of the globe with respect to distance (spread) a dot (cross) is inserted in the respective rectangle.

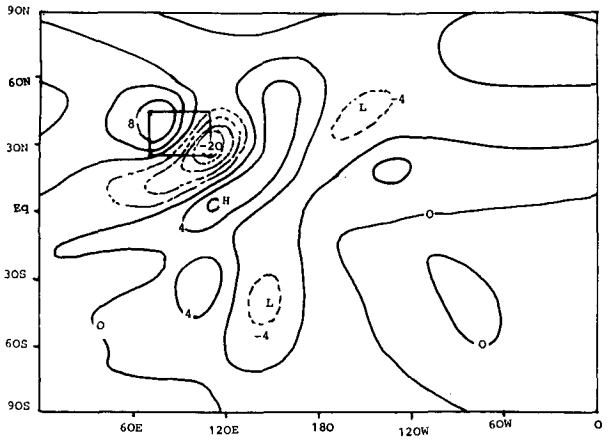

FIG. 5. Sample mean streamfunction $\bar{\psi}_d^{18}$ (10^6 m^2 s^{-1}) in experiment 1 [$\gamma = 1$; $\psi_b = \bar{\psi}_{bz}^1(\varphi)$; $D = 5 \times 10^5$ m^2 s^{-1}; mountain forcing]. The location of the mountain is marked by a rectangle.

imum height $h_0 = 1500$ m is chosen such that the resulting quasi-stationary waves have realistic amplitudes near the mountain, i.e., the corresponding height deviations will fall in the range 100–200 m. The forcing is now more intense than in the foregoing section. Maximum values are $F_d = 2.5 \times 10^{-10}$ s^{-2}. We begin with a series of high-viscosity experiments ($D = 5 \times 10^5$ m^2 s^{-1}).

a. *Experiment 1:* $\bar{\psi}_{bz}^1$; $\gamma = 1$; $D = 5 \times 10^5$ m^2 s^{-1}

The sample mean $\bar{\psi}_d^{18}$ (Fig. 5) shows the familiar pattern of an upstream ridge and a lee-trough to the southeast of the obstacle followed by an arcshaped domain of positive deviations. Wave amplitudes are $\sim 10^7$ m^2 s^{-1} near the mountain. The basic features of this pattern have been explained in relatively simple terms (e.g., Hoskins and Karolyi 1981; Branstator 1983). Note, however, that we include here the interaction of the deviation flow with the mountain, i.e., we retain the term $J(\psi_d, 2\Omega \sin\varphi_0 h/H)$ in (2.9). This term is excluded in most linear theories of mountain induced Rossby waves. We observe closed isolines in the Southern Hemisphere. Although there is a narrow belt of easterlies in the observed flow field at the equator the linear model predicts wave perturbations to the south of these easterlies. This may be due to transience since the model equations never reach a state of complete stationarity. Thus, wave propagation through the equatorial easterlies is possible. However, the model's low resolution may be also responsible for this effect. We cannot expect that waves are completely blocked by critical lines in a model with just ten wavenumbers in meridional direction (Nigam 1985).

Due to the increase in the forcing intensity the deviation energies are now about three times as large as in experiment 1 of the foregoing section (see Tables 1 and 2). Nevertheless individual monthly means exhibit a strong similarity to Fig. 5 which is reflected in the large values of the pattern correlation coefficients p (Table 2).

b. *Experiment 2:* $\bar{\psi}_{bz}^1$; $\gamma = 0$; $D = 5 \times 10^5$ m^2 s^{-1}

In this experiment we just add the nonlinear term $J(\psi_d, \nabla^2\psi_d)$ to (2.6). The sample mean field (not shown) is quite similar to Fig. 5 although both the upstream ridge and the lee-trough are slightly more intense now. This indicates that the quasi-stationary waves in experiment 2 are able to extract more energy from the interaction of the background flow with the mountain than in the linear experiment (see also Table 2). The correlation coefficients between Fig. 5 and the monthly mean fields in this experiment are in the range $0.72 \leq p \leq 0.82$ (Table 2). The PB-test reveals that the experiments tend to differ with respect to either distance or spread over most of the Northern Hemisphere. There is more agreement to the south of the equator (Fig. 6). This means that nonlinear effects cause a statistically significant deviation from the linear solution at least near the source. This result appears to contradict to some extent our earlier result as displayed in Fig. 4. We have to keep in mind, however, that the situation in Fig. 6 differs fundamentally from that tested earlier. Now, we have flows with very little transience. Thus, the scatter in each experiment is small and nonlinear effects can come out clearly. In Fig. 4, the PB-test is applied to samples with large scatter. Then, nonlinear effects are hard to detect in the noisy samples.

c. *Experiment 3:* $\psi_{bz}(\varphi, t)$; $\gamma = 0$; $D = 5 \times 10^5$ m^2 s^{-1}

We find from Table 2 that the time variability of the zonal flow induces no enhancement of the energy of

TABLE 2. Average energies in (m^2 s^{-2}) of the daily fields $E(\psi_d)$, of the monthly means $E(\bar{\psi}_d^1)$ and the energy of the sample mean $E(\bar{\psi}_d^{18})$ and the range of the pattern correlation coefficients p and p_L in experiments 1–5; $D = 5 \times 10^5$ m^2 s^{-1}; $C = 1/(10$ days); mountain forcing.

Experiment	$E(\psi_d)$	$E(\bar{\psi}_d^1)$	$E(\bar{\psi}_d^{18})$	p	p_L
1	25	24	23	$0.95 \leq p \leq 0.98$	—
2	31	30	29	$0.94 \leq p \leq 0.99$	$0.72 \leq p_L \leq 0.82$
3	30	29	28	$0.92 \leq p \leq 0.99$	$0.71 \leq p_L \leq 0.81$
4	27	26	22	$0.86 \leq p \leq 0.97$	$0.55 \leq p_L \leq 0.73$
5	44	26	22	$0.73 \leq p \leq 0.96$	$0.53 \leq p_L \leq 0.79$

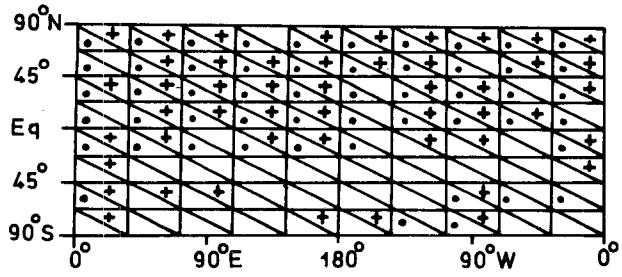

FIG. 6. Intercomparison of the 18 monthly means of experiments 1 and 2 ($D = 5 \times 10^5$ m^2 s^{-1}; mountain forcing) on the basis of the PB-test. If the experiments differ at the 95% level in a subsection of the globe with respect to distance (spread) a dot (cross) is inserted in the respective rectangle.

the deviation field as compared to experiment 2. The monthly mean maps in this experiment are almost replicas of those obtained in experiment 2. Both experiments have been compared on the basis of the PB-test. No difference has been found. This result corroborates the finding of Egger (1984) that the long-term variability induced by the time dependence of mean zonal flow impinging at mountains is small.

d. Experiment 4: $\bar{\psi}_b^1(\lambda, \varphi)$; $\gamma = 0$; $D = 5 \times 10^5$ m^2 s^{-1}

The energy level of the deviation field decreases slightly when a zonally varying background flow is prescribed (Table 2). As in Table 1, the energy of the daily fields is hardly changed when compared to experiments 1–3. The sample mean field (not shown) shows good similarity to Fig. 5 ($p_L = 0.71$). Individual months may differ considerably however from the sample mean (Table 2). As an example we show in Fig. 7 the monthly mean for February 1982. In this month the

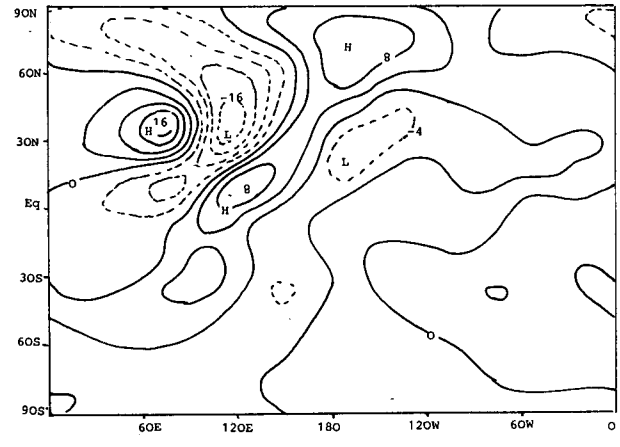

FIG. 7. Monthly mean streamfunction $\bar{\psi}_d^1$ (10^6 m^2 s^{-1}) for February 1982 in experiment 4 [$\gamma = 0$; $\bar{\psi}_b^1(\lambda, \varphi)$ $D = 5 \times 10^5$ m^2 s^{-1}; mountain forcing].

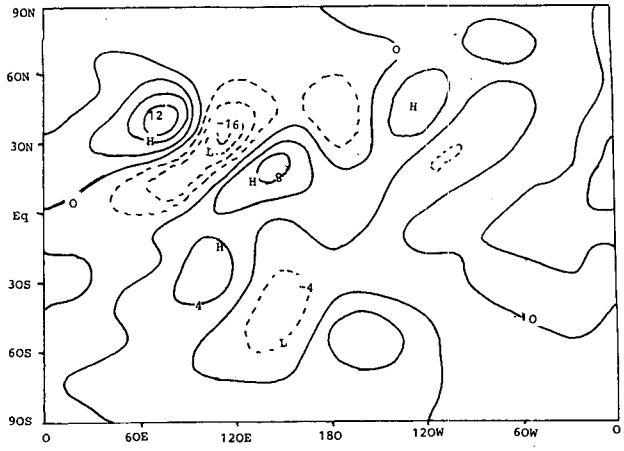

FIG. 8. Monthly mean streamfunction $\bar{\psi}_d^1$ (10^6 m^2 s^{-1}) for January 1981 in experiment 5 [$\gamma = 0$; $\psi_b(\lambda, \varphi, t)$; $D = 5 \times 10^5$ m^2 s^{-1}; mountain forcing].

lee-trough is extremely well developed. Note the large center of positive ψ_d near the pole which is absent in the sample mean. With $0.55 \leq p_L \leq 0.73$ the linear theory is of rather limited value in explaining the computed monthly mean fields. All these results are quite similar to those obtained in the experiment 4 with a localized vorticity source.

e. Experiment 5: $\psi_b(\lambda, \varphi, t)$; $\gamma = 0$; $D = 5 \times 10^5$ m^2 s^{-1}

The sample mean field (not shown) is quite similar to Fig. 5 although details differ. Visual scanning of monthly mean maps reveals good similarity to Fig. 5 near the mountain. In Fig. 8, we show the mean for January 1981 where we find all the familiar features of the standing quasi-stationary linear wave field near the mountain. However, there is no similarity at all to Fig. 5 in the western hemisphere. The linear theory can hardly explain more than 30–40 percent of the monthly means. The PB-test reveals that experiments 1 and 5 differ almost everywhere with respect to spread and distance except a few areas in the Southern Hemisphere. The energy $E(\psi_d)$ of the daily fields doubles that of the sample mean. Due to the high eddy viscosity the damping of the transients is more effective now than in the foregoing experiment with a localized vorticity source and $D = 1 \times 10^5$ m^2 s^{-1}.

We turn now to the last series of experiments where again a reduced eddy viscosity $D = 1 \times 10^5$ m^2 s^{-1} is prescribed. Note that this is still a relatively large value. For example, Simmons et al. (1983) use a fourth-order diffusion with a coefficient 2×10^{16} m^4 s^{-1} (see also Branstator 1983). This kind of damping would be completely ineffective at the scales retained in our computations. We perform only experiments 1, 4 and 5.

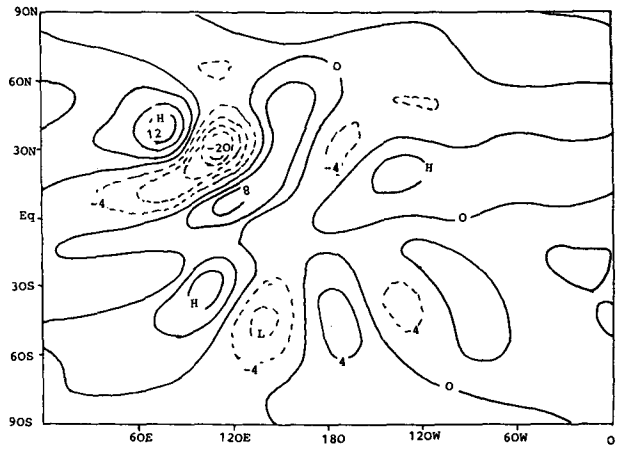

FIG. 9. Sample mean $\bar{\psi}_d^{18}$ (10^6 m^2 s^{-1}) in experiment 1 [$\gamma = 1$; $\bar{\psi}_{bz}^1(\varphi)$; $D = 1 \times 10^5$ m^2 s^{-1}; mountain forcing].

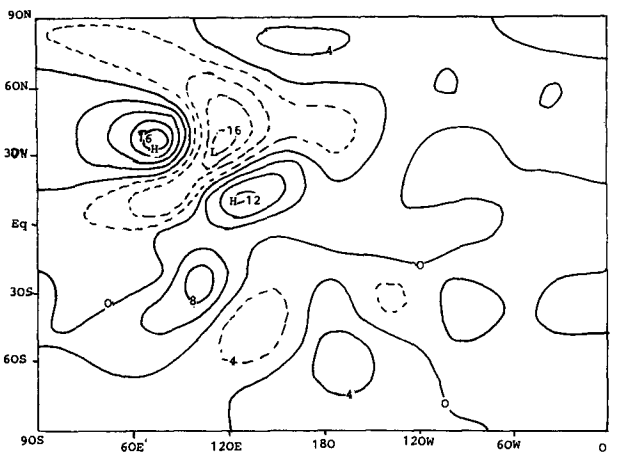

FIG. 10. Sample mean streamfunction $\bar{\psi}_d^{18}$ (10^6 m^2 s^{-1}) in experiment 4 [$\gamma = 0$; $\bar{\psi}_b^1(\lambda, \varphi)$; $D = 1 \times 10^5$ m^2 s^{-1}; mountain forcing].

f. Experiment 1: $\bar{\psi}_{bz}^1(\varphi)$; $\gamma = 1$; $D = 1 \times 10^5$ m^2 s^{-1}

We show the sample mean of the linear runs in Fig. 9. As one would have expected, Fig. 9 is fairly similar to Fig. 5. The wave system near the mountain has somewhat larger amplitudes now and the flow in the Southern Hemisphere is also more energetic. The energy $E(\bar{\psi}_d^{18})$ of the sample mean is 33 m^2 s^{-2} as compared to 23 m^2 s^{-2} in Fig. 5 (Table 3). The variability of the monthly means is larger than in the high viscosity case. Nevertheless individual monthly mean maps are so similar to Fig. 9 that we do not show an example.

g. Experiment 4: $\bar{\psi}_b^1(\lambda, \varphi)$; $\gamma = 0$; $D = 1 \times 10^5$ m^2 s^{-1}

The sample mean (Fig. 10) is less energetic than that of experiment 1 as was the case for the large eddy viscosity experiments. The lee-trough is fairly extended in this experiment. However, there is little wave energy in the far field. In particular, there is almost no response in the western hemisphere. The energy $E(\psi_d)$ of the daily fields is only slightly larger than in experiment 1.

In Fig. 11 we show the mean streamfunction for February 1982. This map deviates considerably from the sample mean, particularly in the Northern Hemisphere. The correlation with the sample mean may be as low as 0.48, and the linear theory is hardly capable of describing situations like those depicted in Fig. 11 ($0.48 \leq p_L \leq 0.63$; Table 3). The PB-test says that experiments 1 and 4 are different with respect to distance and spread almost everywhere.

h. Experiment 5: $\psi_b(\lambda, \varphi, t)$; $\gamma = 0$; $D = 1 \times 10^5$ m^2 s^{-1}

The energy $E(\psi_d)$ of the daily fields is 175 m^2 s^{-2} in this experiment. This value is close to that of the observed fields ($E \sim 200$ m^2 s^{-2}) and is about four times the value obtained in the high viscosity case. The observed daily fields provide a source of energy to the deviation fields which must be balanced by frictional losses. If D is decreased from 5 to 1 ($\times 10^5$ m^2 s^{-1}) we must expect a corresponding increase of E by a factor ~ 5. The sample mean (Fig. 12), however, has a surprisingly low energy level even in this experiment and shows all the features familiar from the linear solution except for the center of positive ψ_d at 60°N, 150°W. The correlation of Fig. 9 and Fig. 12 is 0.63 which is slightly better than that of any of the individual monthly means. However p_L can be as low as 0.31. This means that the linear theory is not applicable to monthly means in this experiment. This conclusion is supported by the PB-test. An intercomparison of experiments 1 and 5 shows different spread and distance almost everywhere except in some areas in the Southern

TABLE 3. Average energies in (m^2 s^{-2}) of the daily fields $E(\psi_d)$, of the monthly means $E(\bar{\psi}_d^1)$ and energy of the sample mean $E(\bar{\psi}_d^{18})$ and the range of the pattern correlation coefficients p and p_L in experiments 1, 4, 5 with $D = 1 \times 10^5$ m^2 s^{-1}; $C = 1/(10$ days); mountain forcing.

Experiment	$E(\psi_d)$	$E(\bar{\psi}_d^1)$	$E(\bar{\psi}_d^{18})$	p	p_L
1	37	35	33	$0.88 \leq p \leq 0.98$	—
4	45	39	32	$0.84 \leq p \leq 0.93$	$0.48 \leq p_L \leq 0.63$
5	175	52	30	$0.51 \leq p \leq 0.84$	$0.31 \leq p_L \leq 0.62$

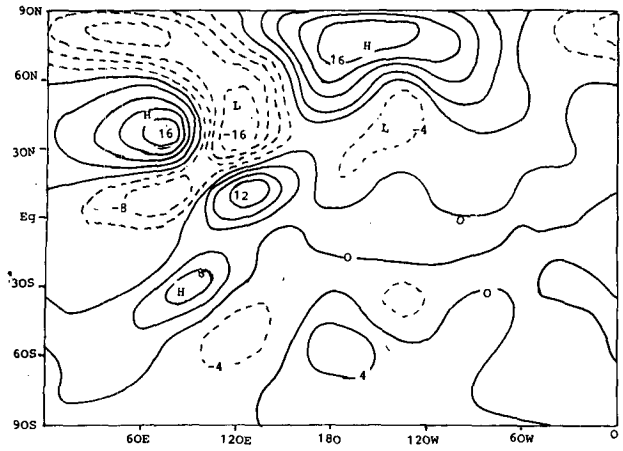

FIG. 11. Monthly mean streamfunction $\bar{\psi}_d^1$ (10^6 m^2 s^{-1}) for February 1982 in experiment 4 ($D = 1 \times 10^5$ m^2 s^{-1}; mountain forcing).

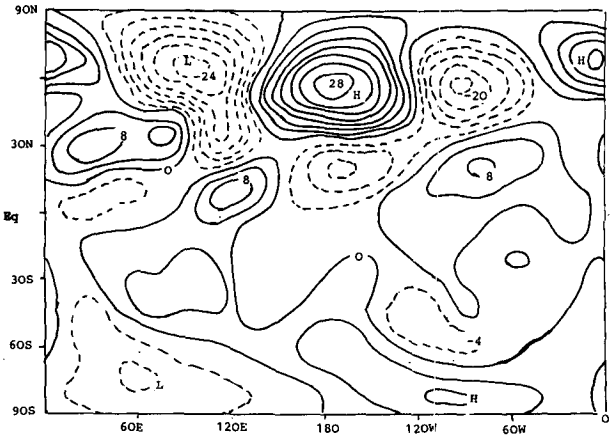

FIG. 13. Monthly mean streamfunction $\bar{\psi}_d^1$ (10^6 m^2 s^{-1}) for February 1981 in experiment 5 ($D = 1 \times 10^5$ m^2 s^{-1}; mountain forcing).

Hemisphere. One could argue that the linear theory would do better if we restrict the intercomparison to areas near the mountain. Indeed if we consider monthly means within a circle of 5000 km radius centered at the Himalayas we find $0.49 \leqslant p_L \leqslant 0.86$. Thus the linear theory may be useful close to the source but not at large distances. In Fig. 13 we show the mean map for February 1981 as an example. There is little similarity to the linear solution nor to the sample mean. The Northern Hemisphere shows a pronounced wave structure where the mountain area is no longer a distinct center of activity. One can still recognize the upstream high and remnants of the trough in the lee. However one would not guess that a mountain near the Himalayas is the "cause" of this deviation field. Correspondingly p can be as low as 0.51 and we have to conclude that the transient eddy forcing shows a large variability at monthly time scales.

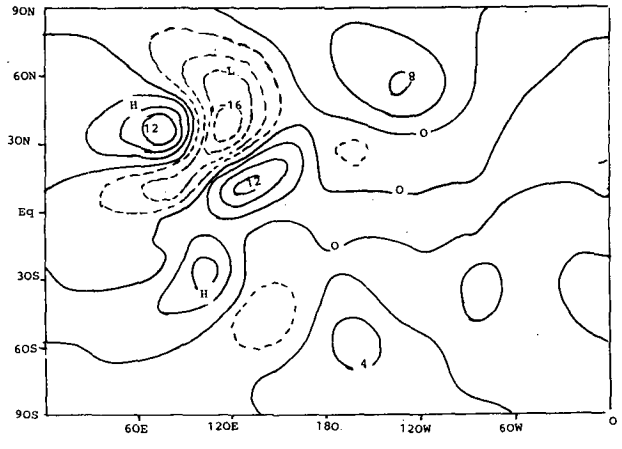

FIG. 12. Sample mean streamfunction $\bar{\psi}_d^{18}$ (10^6 m^2 s^{-1}) in experiment 5 [$\gamma = 0$; $\psi_b(\lambda, \varphi, t)$; $D = 1 \times 10^5$ m^2 s^{-1}; mountain forcing].

5. Critique and conclusion

In this paper we have tested the assumption that the time-dependence of atmospheric flows can be neglected in theories of the quasi-stationary atmospheric response to localized forcing. Before drawing conclusions we briefly want to discuss some of the problems inherent to our approach.

a. Resolution

There is ample evidence in the literature that the resolution $M = N = 10$ chosen here may be insufficient for the computation of steady responses or for the calculation of barotropic instabilities. According to Nigam (1985), for example, a latitudinal resolution of 2–3 deg is required for a satisfactory computation of orographically induced stationary Rossby waves. However, we found that $E(\psi_d) \sim E(\psi_b)$ in experiment 5 with $D = 1 \times 10^5$ m^2 s^{-1}. A further decrease of D to values as prescribed by Nigam [1985; $C = 1/(13.5$ days); $D = 0$] leads to meaningless results (Fig. 15). On the other hand if we keep D near 1×10^5 m^2 s^{-1} it is at least doubtful if Nigam's results still apply. Spectra of the response have been evaluated. They show clearly that most of the deviation energy is concentrated at small wavenumbers. High wavenumbers ($m + r \gtrsim 15$) contain relatively little energy. This suggests that our resolution is sufficient given the relatively high damping rates.

b. Intraseasonal effects

So far we have not commented on trends within one winter. December means differ systematically from February means. There are at least two reasons for these intraseasonal trends. First, the background flow changes its characteristics during the winter and so must the response. This means, in particular, that the mountain forcing has a seasonal trend. Second, the instabilities have relatively small growth rates, mainly

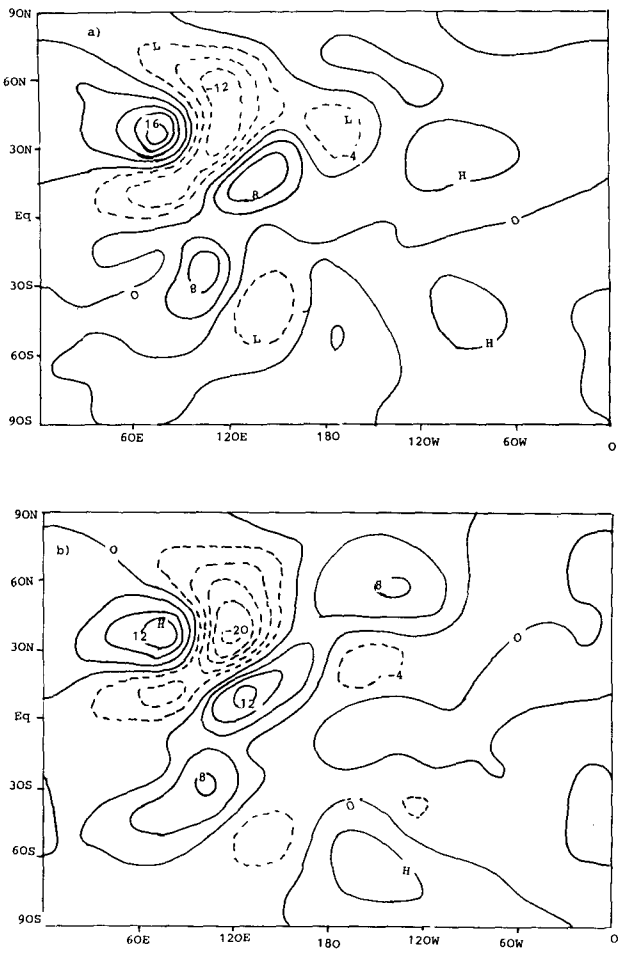

FIG. 14. Monthly mean streamfunction $\bar{\psi}_d^1$ (10^6 m^2 s^{-1}) as obtained by averaging over all days in (a) December and (b) February in experiment 5 ($D = 1 \times 10^5$ m^2 s^{-1}; mountain forcing).

because the damping is so strong. Correspondingly the flow does not completely equilibrate in December. For example the evaluation of $E(\psi_d)$ in experiment 5 ($D = 1 \times 10^5$ m^2 s^{-1}; mountain forcing) gave 94 m^2 s^{-2} on average for all days in December, 195 m^2 s^{-2} in January and 235 m^2 s^{-2} in February. The trend for the monthly means is weaker. We find $E(\bar{\psi}_d^1) = 36$ m^2 s^{-2} in December, 56 m^2 s^{-2} in January and 61 m^2 s^{-2} in February. In Fig. 14 we show the December and February mean maps obtained in experiment 5 in the low viscosity case. It is seen that the wave system near the mountain is more energetic in February. There is little similarity in the far field. However, the overall similarity of both figures is good. We want to stress that the intraseasonal trend is particularly pronounced in this experiment with its low damping rates and the strong input of energy from the background flow. The trend is much smaller in all the other experiments.

c. *Relation to predictability and turbulence studies*

The experiments described in this paper are closely related to work on predictability and error growth in barotropic fluids where one typically considers pairs of numerical predictions with slightly differing initial conditions. These differences grow in turbulent flow and after some time (the predictability time) the pair differs as much as a pair of random realizations. Although the results are model dependent, predictability times of two–three weeks have been found (e.g., Lorenz 1969; Vallis 1985). In our case, we induce deviations from the observed flow by the forcing. These deviations grow in the macroturbulent background flow and may become as energetic as the background flow after some time.

To obtain an estimate for our flow situation we have rerun the mountain experiment 5 for one winter with $D = 0$, $C = 0$. It is found that the growth of the deviation energy is extremely rapid (Fig. 15) and we find a predictability time of about two weeks in agreement with earlier work. We have also computed the energy growth in experiment 4 but with $C = D = 0$. We find in agreement with Simmons et al. (1983) that wavy stationary background flows are unstable with a predictability time of about three weeks. It is sufficient to prescribe $C = 1/(10$ days), $D = 0$, however, in experiment 4 to obtain quick equilibration (see also Simmons et al. 1983), whereas experiment 5 does not reach a stationary energy level for this choice of the parameters within one winter (Fig. 15). These results shed some light on the main problems inherent in our approach. The supply of energy to the error field is limited in the atmo-

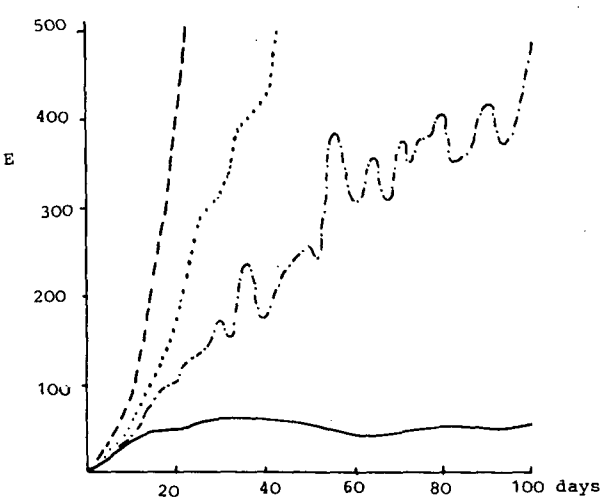

FIG. 15. Energy $E(\psi_d)$ in (m^2 s^{-2}) in the winter 1984/85 in experiments with small friction parameters. Dashed: experiment 5 except with $C = D = 0$. Dotted: experiment 4 except with $C = D = 0$. Dash-dotted: experiment 5 except with $C = 1/10$ days^{-1}, $D = 0$. Solid: experiment 4 except with $C = 1/(10$ days); $D = 0$. Mountain forcing.

sphere and in most of the predictability studies mentioned. Thus the error fields must equilibrate even for inviscid flows. In our experiments the background flow provides an unlimited reservoir of energy. A balance at realistic energy levels can be achieved only by prescribing a strong damping. This shortcoming is the price we have to pay for using observed background flows.

d. *Transient eddy forcing*

It has been found in all experiments 5 that the individual monthly means show a distinct variability while the sample mean is relatively close to the linear sample mean. According to (2.7) the mean "response" to the transient eddy forcing F_t varies strongly at monthly time scales but contains little energy for T = 18 months. To see if this result is realistic we have to turn to data. There is the problem that one cannot relate observed transient eddy activities to some localized forcing as is possible in our experiments. We can, however, check the plausibility of our result by consulting the model of Egger and Schilling (1983). These authors considered the barotropic vorticity equation and determined the response of modes ψ^m_{m+r} to observed transient eddy forcing. The power spectrum of the response shows a pronounced peak at periods of 1–2 months and is essentially white for longer periods. If we average the response over intervals of length T the power spectrum is modified by a factor $[2\sin(\omega T/2)/\omega T]^2$. If T equals one month a considerable fraction of the response's variability is located at periods $> T$ and, therefore, monthly means show a considerable variability. If, however, T = 18 months little variability is located at longer periods. Thus long-term means of the response contain relatively little energy in good agreement with our result.

Given these caveats we now want to draw the conclusions which appear not to be sensitive to the specific choice of the midlatitude forcing. We found about the same type of response for strong mountain forcing and for a relatively weak vorticity source.

1) The forcing induces pronounced transience of ψ_d if the most general background flow (experiment 5) is admitted. This transience as quantified by the transient eddy forcing causes the monthly means to deviate strongly from results of the linear theory. Thus conventional steady-state calculations with $F_t = 0$ cannot be applied to cases where the averaging period is shorter or equal to a season.

2) Conventional linear (or nonlinear) steady-state calculations with $F_t = 0$ become meaningful when T is greater than 10 months, say.

3) If observed monthly means are prescribed as background flows (experiment 4) the growth of deviation energy is greatly reduced as compared to experiments 5. Nevertheless monthly means of ψ_d deviate considerably from linear results.

4) The time variability of the zonal flow (experiment 3) is of little importance to the quasi-stationary Rossby waves.

5) The deviations induced by the forcing grow in observed flow at 300 hPa with daily resolution in time with an e-folding time of about three days and a predictability time of two weeks in the inviscid case. Relatively large damping rates are necessary to achieve an equilibration with $E(\psi_d) \leqslant E(\psi_b)$. Although the linear theories are more successful for $D = 10^5\ \mathrm{m^2\ s^{-1}}$ where $E(\psi_d) \sim 0.2E(\psi_b)$ the results obtained for $D = 1 \times 10^5\ \mathrm{m^2\ s^{-1}}$ where $E(\psi_d) \sim E(\psi_b)$ are most pertinent to the problem of the applicability of linear theories.

Acknowledgments. The author is grateful to G. Müller for evaluating the streamfunction from the wind data and to the referees for their constructive criticism.

REFERENCES

Branstator, G., 1983: Horizontal eddy propagation in a barotropic atmosphere with meridional and zonal structure. *J. Atmos. Sci.*, **40**, 1689–1708.

Charney, J., and A. Eliassen, 1949: A numerical method for predicting the perturbations of the middle latitude westerlies. *Tellus*, **1**, 38–54.

Egger, J., 1977: On the linear theory of the atmospheric response to sea surface temperature anomalies. *J. Atmos. Sci.*, **34**, 603–614.

——, 1984: Stochastic orographic forcing of barotropic β-plane flow. *Tellus*, **36A**, 147–156.

——, and H.-D. Schilling, 1983: On the theory of the long-term variability of the atmosphere. *J. Atmos. Sci.*, **40**, 1073–1085.

Gill, A., 1980: Some simple solutions for heat induced tropical circulation. *Quart. J. Roy. Met. Soc.*, **106**, 447–462.

Held, I., 1983: Stationary and quasi-stationary eddies in the extratropical troposphere: Theory. *Large-Scale Dynamical Processes in the Atmosphere*, I. B. Hoskins and R. Pearce, Eds., Academic Press, 127–168.

Hoskins, B., and D. Karolyi, 1981: The steady linear response of a spherical atmosphere to thermal and orographic forcing. *J. Atmos. Sci.*, **38**, 1179–1186.

Jacqmin, D., and R. Lindzen, 1985: The causation and sensitivity of the Northern winter planetary waves. *J. Atmos. Sci.*, **42**, 724–745.

Lorenz, E., 1969: The predictability of flow which possesses many scales of motion. *Tellus*, **21**, 289–307.

Nigam, S., 1985: On the adequacy of meridional resolution of linear and quasi-linear barotropic models. *J. Atmos. Sci.*, **42**, 2493–2505.

Preisendorfer, R., and T. Barnett, 1983: Numerical model–reality intercomparison tests using small-sample statistics. *J. Atmos. Sci.*, **40**, 1884–1896.

Simmons, A., J. Wallance and G. Branstator, 1983: Barotropic waves propagation and instability, and atmospheric teleconnections. *J. Atmos. Sci.*, **40**, 1363–1392.

Smagorinsky, J., 1953: The dynamical influence of large-scale heat sources and sinks on the quasi-stationary mean motions of the atmosphere. *Quart. J. Roy. Meteor. Soc.*, **79**, 342–366.

Vallis, G., 1984: Baroclinic and barotropic predictability in geostrophic turbulence. *Predictability of Fluid Motions*, G. Holloway and B. West, Eds., Amer. Inst. Phys.